Eur Spine J (2006) 15:1785–1795
DOI 10.1007/s00586-006-0158-0

ORIGINAL ARTICLE

The effect of osteoporotic vertebral fracture on predicted spinal loads in vivo

Andrew M. Briggs · Tim V. Wrigley · Jaap H. van Dieën · Bev Phillips · Sing Kai Lo · Alison M. Greig · Kim L. Bennell

Received: 22 January 2006 / Revised: 16 April 2006 / Accepted: 28 May 2006 / Published online: 4 July 2006

Abstract The aetiology of osteoporotic vertebral fractures is multi-factorial, and cannot be explained solely by low bone mass. After sustaining an initial vertebral fracture, the risk of subsequent fracture increases greatly. Examination of physiologic loads imposed on vertebral bodies may help to explain a mechanism underlying this fracture cascade. This study tested the hypothesis that model-derived segmental vertebral loading is greater in individuals who have sustained an osteoporotic vertebral fracture compared to those with osteoporosis and no history of fracture. Flexion moments, and compression and shear loads were calculated from T2 to L5 in 12 participants with fractures (66.4 ± 6.4 years, 162.2 ± 5.1 cm, 69.1 ± 11.2 kg) and 19 without fractures (62.9 ± 7.9 years, 158.3 ± 4.4 cm, 59.3 ± 8.9 kg) while standing. Static analysis was used to solve gravitational loads while muscle-derived forces were calculated using a detailed trunk muscle model driven by optimization with a cost function set to minimise muscle fatigue. Least squares regression was used to derive polynomial functions to describe normalised load profiles. Regression co-efficients were compared between groups to examine differences in loading profiles. Loading at the fractured level, and at one level above and below, were also compared between groups. The fracture group had significantly greater normalised compression ($p = 0.0008$) and shear force ($p < 0.0001$) profiles and a trend for a greater flexion moment profile. At the level of fracture, a significantly greater flexion moment ($p = 0.001$) and shear force ($p < 0.001$) was observed in the fracture group. A greater flexion moment ($p = 0.003$) and compression force ($p = 0.007$) one level below the fracture, and a greater flexion moment ($p = 0.002$) and shear force ($p = 0.002$) one level above the fracture was observed in the fracture group. The differences observed in multi-level spinal loading between the groups may explain a mechanism for increased risk of subsequent vertebral fractures. Interventions aimed at restoring vertebral morphology or reduce thoracic curvature may assist in normalising spine load profiles.

Keywords Osteoporosis · Vertebral fracture · Spine loading · Biomechanics · Optimization

A. M. Briggs (✉) · T. V. Wrigley · A. M. Greig · K. L. Bennell
Centre for Health, Exercise and Sports Medicine, School of Physiotherapy, University of Melbourne, 200 Berkeley Street, Parkville, VIC 3010, Australia
e-mail: briggsam@unimelb.edu.au

K. L. Bennell
e-mail: k.bennell@unimelb.edu.au

B. Phillips
Rehabilitation Sciences Research Centre, School of Physiotherapy, University of Melbourne, 200 Berkeley Street, Parkville, VIC 3010, Australia

A. M. Briggs · A. M. Greig
Department of Medicine, Royal Melbourne Hospital, University of Melbourne, Parkville, VIC 3010, Australia

J. H. van Dieën
Institute for Fundamental and Clinical Human Movement Sciences, Faculty of Human Movement Sciences, Vrije Universiteit, Van der Boechorststraat 9, 1081 BT Amsterdam, The Netherlands

S. K. Lo
Faculty of Health and Behavioural Sciences, Deakin University, Burwood, VIC 3125, Australia

Introduction

Vertebral fractures are recognised as the hallmark of osteoporosis and represent a significant burden to the individual and public health system worldwide. Once an incident vertebral fracture is sustained, the risk of subsequent fracture increases significantly, even within the first year [38]. Previous studies report the risk of sustaining a vertebral fracture to increase by four to sevenfold after an initial fracture, and then exponentially with greater numbers of prior vertebral fractures [3, 36, 44, 45]. This scenario has been termed the 'vertebral fracture cascade'. Despite many investigations into the morbidities and efficacy of pharmacologic agents associated with osteoporotic vertebral fractures, the mechanisms underlying fracture and subsequent fracture aetiology are inadequately understood.

Many factors may contribute to the increased fracture risk such as trunk neuromuscular control, lifestyle changes and bone quality changes [5, 29]. It is likely that this observed fracture cascade is due, in part, to changes in physiologic loading of the spine. Reduced anterior vertebral height, as a consequence of wedge fracture, will increase the angle of superior endplate tilt and thus contribute to anterior translation of the centre of mass (COM) of the trunk. The shift in COM will therefore increase the moment arm between the vertebra and COM, contributing to higher flexion moments. In addition, the shear and compression forces imposed on the fractured vertebra, and those adjacent to it, would likely increase as a result of greater paraspinal muscle force and gravitational loading. Notably, such changes have been shown previously in a modelling study [34].

The ability of the spine to withstand physiologic loads depends on material and design properties of the spine, as well as the loading characteristics imposed on the system [5]. Material properties of bone have been explored extensively in the literature, enhancing our understanding of the contribution of bone mineral density (BMD) and trabecular and cortical bone quality to vertebral fracture mechanisms [20, 41, 47]. However, a comprehensive understanding of multi-level physiologic loading in the spine in vivo is lacking. Many studies have examined vertebral bone strength by measuring stress–strain and load-to-failure properties and their associations to BMD. These studies rely on ex vivo designs and/or finite element modelling, and often test a limited number of vertebrae [8, 14–17, 26, 37, 47]. Although findings from ex vivo studies assist in the understanding of fracture mechanics, the results may not accurately represent in vivo behaviour, making them potentially unreliable [35]. Furthermore, deriving results from a limited number of vertebral segments and using uniaxial load models may oversimplify the complex loading profiles that exist in the human spine. Thus, an understanding of the multi-segmental loading *profile* of the spine is important.

Comparing physiologic loading characteristics between spines with and without fractures in vivo may assist in the understanding of fracture mechanics and the clinically observed fracture cascade phenomenon. The aim of the current study was to model and quantitatively compare physiologic loading in vivo in standing, in a population with and without osteoporotic vertebral fracture. We hypothesised that greater segmental flexion moments, compression forces and shear forces would exist in individuals with an osteoporotic vertebral fracture compared to those with osteoporosis and no history of vertebral fracture.

Materials and methods

Participants

Thirty-one elderly, female participants with osteoporosis were recruited from osteoporosis support groups, outpatient clinics, and from the community within the Melbourne metropolitan area via newspaper advertisements. Participants were included on the basis that they had primary osteoporosis, aged at least 50 years and be at least 5 years post-menopausal. Individuals with a history of spinal surgery or vertebroplasty/kyphoplasty were excluded. A diagnosis of osteoporosis was confirmed with bone densitometry *T*-scores derived from dual energy X-ray absorptiometry scans of the hip and/or spine, based on World Health Organisation guidelines (T-score < -2.5) [2]. Participants were divided into two groups—those with a vertebral fracture ($n = 12$) and without ($n = 19$). All participants provided written informed consent and approval to conduct this study was granted by Institutional Review Boards and complied with Australian research laws.

Imaging

Participants adopted their normal, relaxed standing posture against an X-ray plate. Lateral radiographs were captured of the thoracic (T1–T12) and lumbar spines (T12–L5). A radiograph of a radio-opaque ruler in a fixed position, hanging vertically was also taken in thoracic and lumbar images for scaling and transforming vertebral co-ordinate data. In addition, digitised points on the vertically hanging ruler were used to correct for any rotation error in the radiograph plane.

Digital photographs taken at the time of X-ray imaging provided data on the positions and lengths of the head, neck and upper limbs relative to the spine, when expressed in a common co-ordinate system. The camera was positioned 4 m away and perpendicular to the participant to minimise perspective distortion. Markers were attached to anatomical landmarks to define body segment lengths for the upper limbs (head of humerus, lateral humeral epicondyle, ulnar styloid and head of the fifth metacarpal bone), neck (C7 spinous process, tragus) and head (vertex of the skull) [31, 49], as outlined in Fig. 1.

Diagnosis of vertebral fracture

Diagnosis of vertebral fracture was made from the lateral radiographs. A semi-quantitative assessment was used, following guidelines recommended by Genant et al. [23]. Anterior and posterior vertebral heights (H_A and H_P, respectively) of vertebrae T1–L5 were calculated from digitised vertebral co-ordinates. Similar to McCloskey et al. [39], a vertebral body was classified as 'fractured' when two criteria were fulfilled at each site, to reduce the number of false positives. Vertebrae were classified as wedge-fractured if the H_A was reduced by ≥30% compared to its H_P *and* the H_P of the adjacent superior or inferior vertebra. Radiographs were also reviewed qualitatively by a radiologist to ensure that compression and biconcave fractures were not overlooked. Seventeen wedge fractures were identified in the fracture group at vertebral levels T4 (17.6%), T5 (11.8%), T6 (23.5%), T7 (11.8%), T8 (23.5%), T9 (5.9%) and T12 (5.9%). Three patients had sustained more than one vertebral fracture.

Image analysis

Sagittal curvature of the thoracic spine was measured manually using standard radiographic techniques—a Cobb angle between T4 and T9 [25] and a vertebral centroid angle. The latter was defined as the angle between lines intersecting vertebral centroids of T4/5

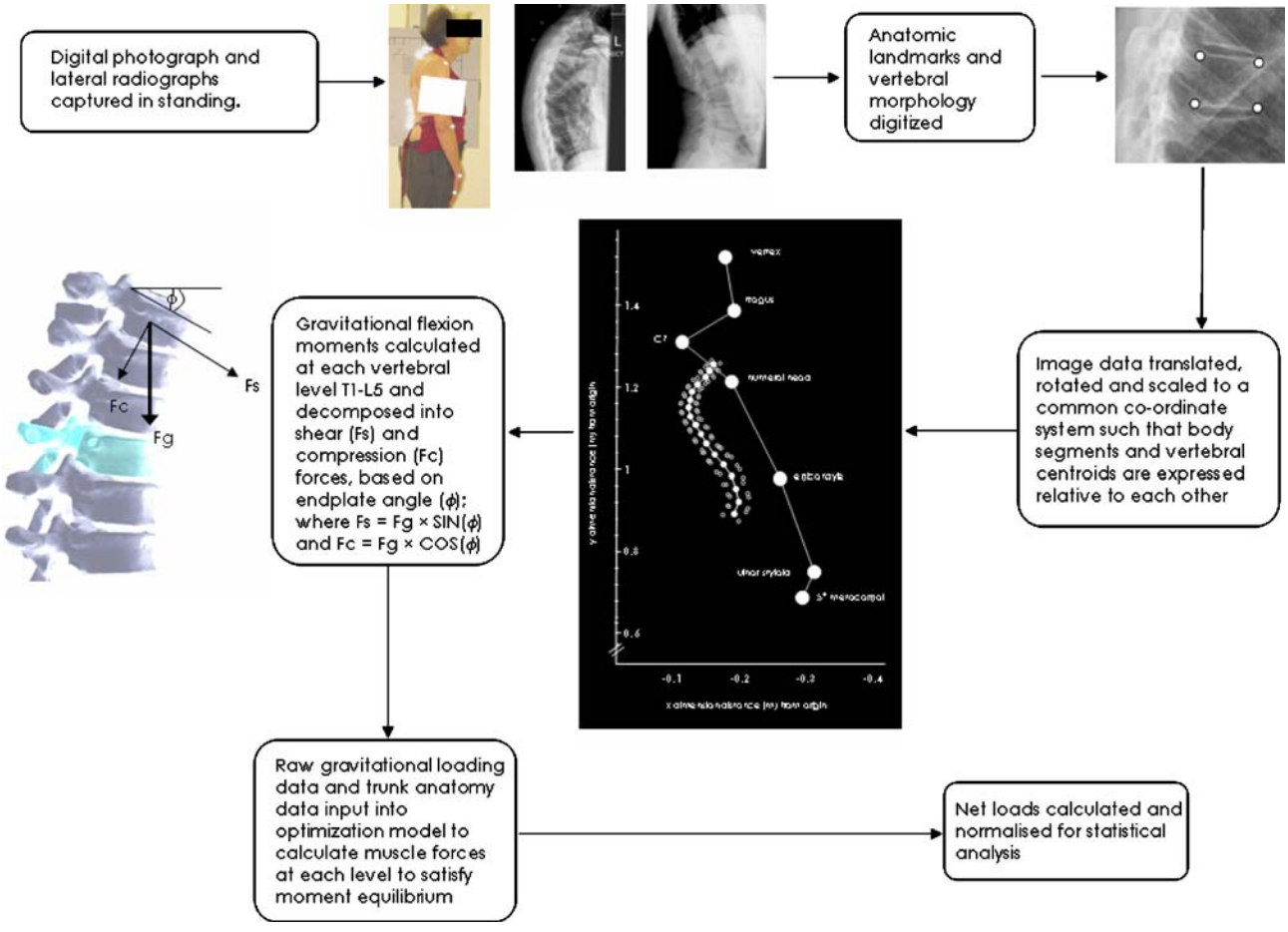

Fig. 1 Schematic representation of steps followed for acquisition and analysis of image data and calculations to derive net loads at each vertebral level

and T8/9 and has been validated previously for the thoracic and lumbar spine [6, 27]. Image analysis software (Image J Version 1.30, NIH, MD, USA) was used to manually digitise x, y co-ordinates of the four vertebral body corners of T1–L5 from the digital radiographs. A study of ten randomly selected films demonstrated excellent intra-rater precision for this process in the thoracic spine (ICC 1,1: 0.98–0.99; %CV: 0.19–0.91%). Vertebral centroid co-ordinates were calculated from the corner co-ordinates (Fig. 1). Co-ordinates of anatomic markers were also digitised from the digital photos, from which segment positions and lengths were calculated. All image data were scaled and transformed to a common co-ordinate system to enable the position of the body segments and vertebral centroids to be expressed relative to each other (Fig. 1). Spinal curvature was also measured intersegmentally (referring to angulation between adjacent vertebral centroids). This was achieved by fitting cubic functions to the profile of vertebral centroid co-ordinates for each participant (R^2 = 0.98–0.99). The gradient of the function at each vertebral level was calculated by differential calculus, and then its angle (θ) solved at each level (Eq. 1).

$$\theta = a\ \tan(\mathrm{d}y/\mathrm{d}x[ax^3 + bx^2 + cx + d]) = a\ \tan(3ax^2 + 2bx + c), \quad (1)$$

where x is the x-co-ordinate of the vertebral centroid and a, b, c are co-efficients and d is the constant term in a cubic function.

Load estimations

Gravitational loads (flexion moments, compression, shear force) were calculated about the vertebral centroids for T1–L5. Data on the COM positions and percentage of total body mass for body segments and each vertebral level were extracted from previously published studies where anthropometric data was comparable to the participants in the current study [31, 42, 49]. In addition, inertial data of the trunk reported by Pearsall et al. [42] was scaled to participant body height. Net segmental flexion moments were calculated as the product of the lever arm distance between a given vertebral centroid and a composite COM position, and the net gravitational force at that level (including superior vertebral levels, head, neck and arms). The gravitational force at each level was decomposed into compression and shear vectors based on the angle of the superior endplate tilt at each level (Fig. 1). Forces produced by trunk muscles were calculated from T2 to L5 using a non-linear optimization routine. Optimization is a common class of biomechanical model used to calculate individual muscle forces from a feasible set to solve an indeterminacy problem, i.e. a highly redundant number of muscle activation patterns could be used to satisfy moment equilibrium. Optimization models attempt to overcome this problem by minimising or maximising a physiologic criterion (cost function), and yield a unique set of muscle forces from a previously indeterminable set. The cost function proposed by Crowninshield and Brand [9] to predict muscle activation with the aim of minimising muscle fatigue was used in the current model, and has been validated for this purpose previously [10, 11]. Skeletal and muscular trunk anatomy input data were derived from a previous study describing 180 muscles [48]. Optimization calculations were performed using the constrained optimization function ('fmincon') in the Matlab 6.5 (The Mathworks Inc., Natick, MA, USA) optimization toolbox, to determine a vector of muscle activation minimising the cost function described above. Moment equilibrium was constrained to all levels of the lumbar spine (T12–L5) and maximal muscle stress was set at 50 N/cm^2. Passive stiffness was modelled with a rigid beam matrix to represent motion segment stiffness based on a finite element analysis of intervertebral motion segments [22]. In this stiffness model, intervertebral rotation and displacement of vertebral body centres were constrained to be $<1°$ and 1 mm, respectively, in all directions. Axial displacements were unconstrained and intervertebral joint contact forces were ignored. Muscle length changes resulting from joint displacements in the stiffness model were predicted to be small and were therefore ignored. Muscle moment estimates were decomposed into shear and compression forces for each vertebral level based on intersegmental angles described previously on a per-participant basis.

Data analysis

Differences in physical characteristics between the fracture and non-fracture groups were explored with independent t-tests. Flexion moments were normalised to body weight (BW) × height (Ht) and compression and shear forces were normalised to BW. Profiles of net segmental load parameters from T2 to L5 and intersegmental angles in each group were described with least squares polynomial regression functions. For both fracture and non-fracture groups, cubic functions were fitted to segmental flexion moments and shear forces, while quadratic regression models described compression forces. Intersegmental angle profiles were described with cubic functions. To compare differences in

net loading profiles and intersegmental angle profiles between fracture and non-fracture groups, corresponding co-efficient terms in the polynomial functions were compared using independent *t*-tests. For the polynomial functions to be considered statistically different, a significant difference between one or more corresponding co-efficient terms was required. Regression functions were plotted to interpret the nature of the differences between groups. This rationale has been used previously and is an accepted statistical approach for hypothesis testing [40]. Paired *t*-tests were used to examine load parameters at the fracture level, and at one level above and one level below the fracture, compared to mean loads at the equivalent levels in the non-fracture group. A single vertebral level (from amongst 2 to 4) was randomly chosen for analysis for participants who had sustained more than one vertebral fracture ($n = 3$). The level of significance was set at $\alpha = 0.05$ (2-tailed).

Results

Descriptive statistics for each group are presented in Table 1. A significant difference in height ($p = 0.03$) and mass ($p = 0.01$) was observed between the groups, with the fracture group being on average 4 cm taller and 10 kg heavier than the non-fracture group. There was no difference in kyphosis when measured by the Cobb or centroid angles ($p = 0.14$ and $p = 0.43$, respectively). Cubic functions explained a significant proportion of the variance ($p < 0.0001$) in segmental curvature for fracture and non-fracture groups ($R^2 = 90.2$ and 89.8%, respectively). The profile of intersegmental angles was significantly different between groups ($p < 0.0001$), where the fracture group demonstrated greater intersegmental curvature (Fig. 2).

Flexion moments

The flexion moment profile in the fracture group demonstrated a trend for systematically greater flexion moments compared to the non-fracture group, with moments peaking in the mid-thoracic spine (Table 2, Fig. 3). However, no significant difference in the flexion moment profile was observed between the groups. The peak mean flexion moment in both groups occurred at T8 with normalised values of 0.018 Nm/BW × Ht in the fracture group and 0.015 Nm/BW × Ht in the non-fracture group. The percentage difference in mean flexion moments between the groups from T1 to L5 ranged from 10.3 to 71.5%.

Compression forces

Normalised compression forces increased from T2 to L4 as a function of vertebral level in the fracture (0.17–0.68 N/BW) and non-fracture (0.17–0.59 N/BW) groups. A significant difference between fracture and non-fracture compression force profiles was established ($p = 0.0008$, Table 2, Fig. 4). The mean compression forces in the fracture group were 1.7–5.4% lower than those of the non-fracture group between T2 and T6 and then greater by 1.1–17.1% between T7 and L5.

Shear forces

A significant difference between fracture and non-fracture shear force profiles was established ($p < 0.0001$, Table 2, Fig. 5). Generally, the mean anterior and posterior shear forces of the fracture group were greater than those of the non-fracture group by 8.1–135.9%. Mean shear forces in the fracture group were lower than those of the non-fracture group at T8, T9, T11, L2, L3 and L5. Normalised anterior shear force was maximal at T3 in both groups (fracture = 0.12 N/BW, non-fracture = 0.10 N/BW). Normalised posterior shear force was maximal at T12 in both groups (fracture = –0.14 N/BW, non-fracture = –0.13 N/BW).

Between-group fracture level comparisons

At the level of fracture, a significantly greater flexion moment ($p = 0.001$) and shear force ($p < 0.001$) was observed in the fracture group of 15.7 and 272.6%, respectively (Fig. 6a, c). There was no significant difference in compression force at the level of fracture (Fig. 6b). At one level below the fracture, a significantly

Table 1 Descriptive statistics of sample characteristics expressed as the mean (SD)

Group	Age (year)	Height (cm)[a]	Mass (kg)[a]	Cobb angle (°)	Centroid angle (°)
Fracture ($n = 12$)	66.4 (6.4)	162.2 (5.1)	69.1 (11.2)	42.5 (9.9)	33.8 (8.1)
Non-fracture ($n = 19$)	62.9 (7.9)	158.3 (4.4)	59.3 (8.9)	37.6 (7.9)	31.4 (8.0)

[a]Significant difference ($p < 0.05$, 2-tailed)

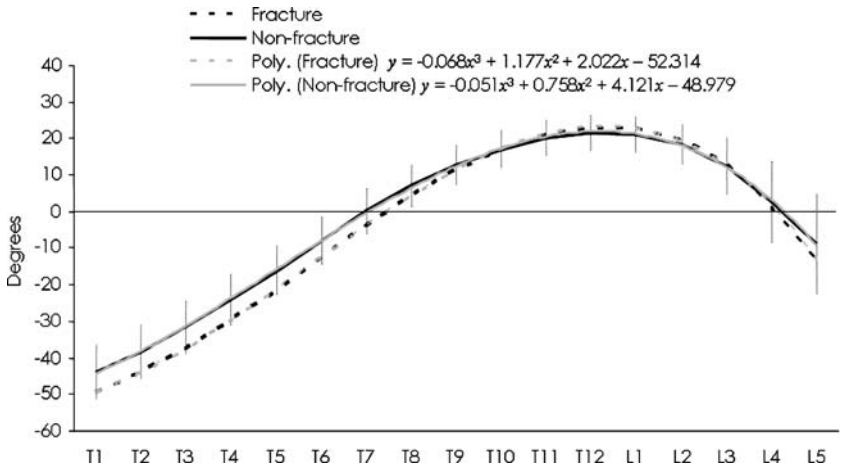

Fig. 2 Mean intersegmental angles of the fracture and non-fracture groups with polynomial functions superimposed as *grey lines*. The 1SD of the non-fracture group is represented by *vertical bars*. The intersegmental angles represent the angle (relative to vertical) of the gradient of the cubic function fitted to the vertebral centroids. Thus, the intervertebral angle represents the angle between adjacent vertebral centroids

Table 2 Details of polynomial functions for each normalised load parameter in each group, and results of *t*-tests between co-efficient terms

Polynomial co-efficients	Flexion moment (Nm/BW × Ht)			Compression force[a] (N/BW)			Shear force[a] (N/BW)		
	Fracture	Non-fracture	*p*-value	Fracture	Non-fracture	*p*-value	Fracture	Non-fracture	*p*-value
x^3	6.58×10^{-6}	0.00001	0.841	–	–	–	0.00068	0.00619	< 0.0001
x^2	–0.00034	–0.00032	0.664	0.00140	0.00093	0.0008	–0.01613	–0.01431	0.070
X	0.00397	0.00361	0.323	0.00905	0.01040	0.627	0.08737	0.07352	0.111
Constant	0.00351	0.00324	0.725	0.14424	0.15563	0.340	–0.00765	–0.00347	0.846
R^2 of regression function	0.53	0.66		0.86	0.89		0.75	0.78	
df[b]	200	319	–	189	301	–	188	300	–

[a]Significant difference ($p < 0.05$, 2-tailed)

[b]Degrees of freedom (residuals)

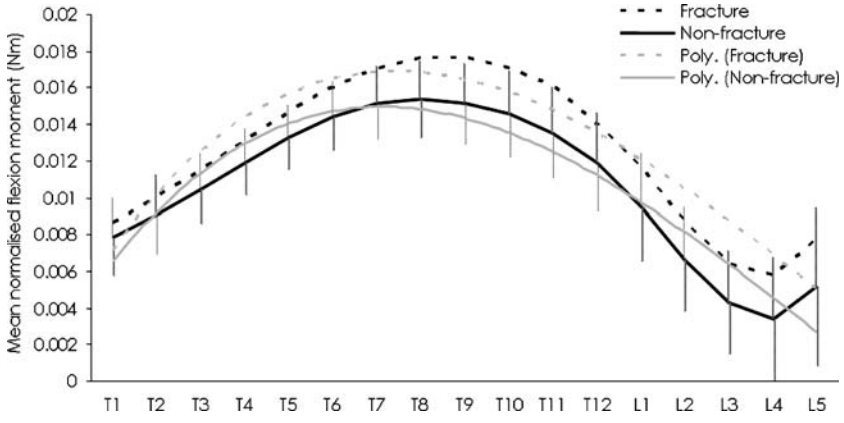

Fig. 3 Normalised flexion moment (Nm/BW × Ht) profiles with 1SD of non-fracture group represented by *vertical bars*. Polynomial functions superimposed as *grey lines* (see Table 2 for co-efficients)

greater flexion moment ($p = 0.003$) and compression force ($p = 0.007$) was observed in the fracture group of 16.8 and 3.7%, respectively, while no significant difference was observed in shear force (Fig. 6a–c). At one level above the fracture, a significantly greater flexion moment ($p = 0.002$) and shear force ($p = 0.002$) was observed in the fracture group of 13.9 and 85.0%, respectively, while no significant difference was observed in compression force between groups (Fig. 6a–c).

Within group fracture level comparisons

For both groups a significant difference in normalised compression (both $p < 0.001$) and shear forces (both $p < 0.001$) were observed between the level of

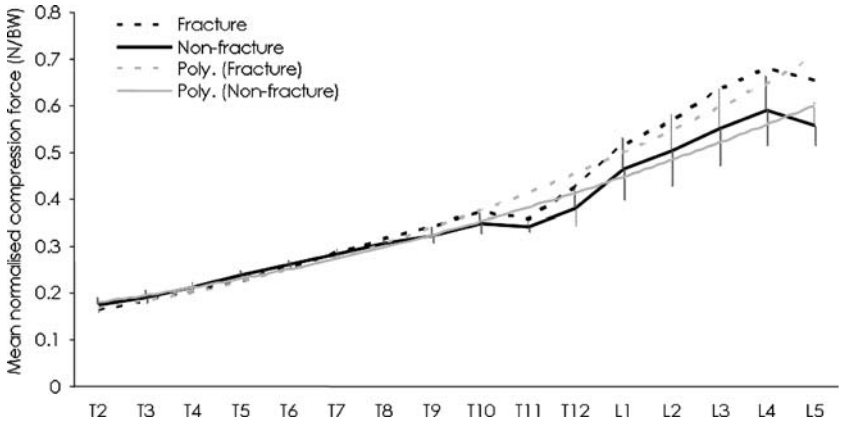

Fig. 4 Normalised compression force (N/BW) profiles with 1SD of non-fracture group represented by *vertical bars*. Polynomial functions superimposed as *grey lines* (see Table 2 for co-efficients)

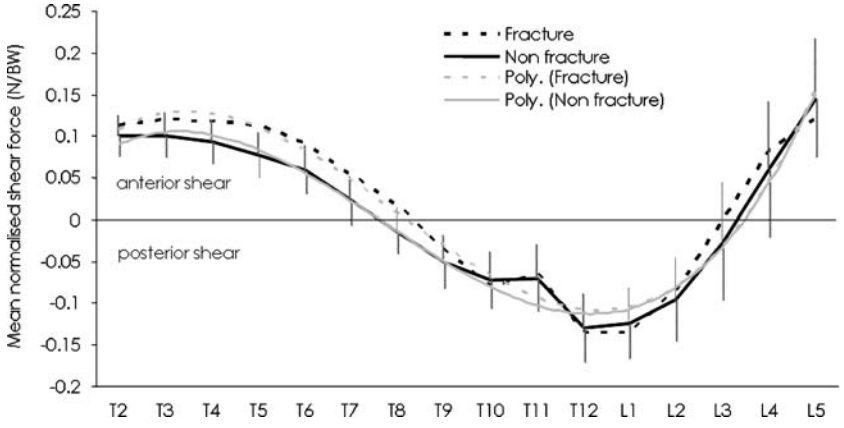

Fig. 5 Normalised shear force (N/BW) profiles. Force above zero represents anterior shear, while below zero represents posterior shear. The 1SD of the non-fracture group is represented by *vertical bars*. Polynomial functions superimposed as *grey lines* (see Table 2 for co-efficients)

fracture and one level below (Fig. 6b, c). There was no difference between these levels for flexion moments in either group. Notably, compared to the fractured level, normalised compression force increased at one level below the fracture by a greater proportion in the fracture group (13.3%) compared to the non-fracture group (9.7%). Normalised anterior shear force decreased from the fractured level to one level below the fracture by 85.9% in the fracture group and by 117.7% in the non-fracture group.

Discussion

This study estimated segmental loading in upright stance through the thoracolumbar spine in vivo in a population with and without osteoporotic vertebral fractures. Estimating load parameters over a number of spinal segments provides a more comprehensive understanding of postural loading through the spine. Notably, individuals who had sustained a vertebral fracture demonstrated significantly greater spinal load profiles compared to those with no history of vertebral fracture. These differences may help to explain the clinically observed vertebral fracture cascade.

Mechanical loading in static situations is directly related to mass distribution and therefore spinal curvature (assuming load data are normalised to mass). The trend towards a larger mean difference between groups based on the Cobb angle was not surprising since this angle is derived principally from endplate tilt and thus would be expected to be greater in cases of wedge fractures. This measurement artefact in the Cobb angle has created uncertainty regarding its validity for quantifying sagittal curvature. Other methods such as the centroid angle have been proposed to overcome the limitations of the Cobb angle [6, 27]. We found no significant difference in thoracic kyphosis between the groups using these standard radiographic measures. However, comparisons of intersegmental curvature profiles showed a difference between groups, suggesting that the differences in loading characteristics between individuals with and without fractures were directly attributable to subtle, yet clinically significant differences in intersegmental curvature. It is important to note that 75% of the

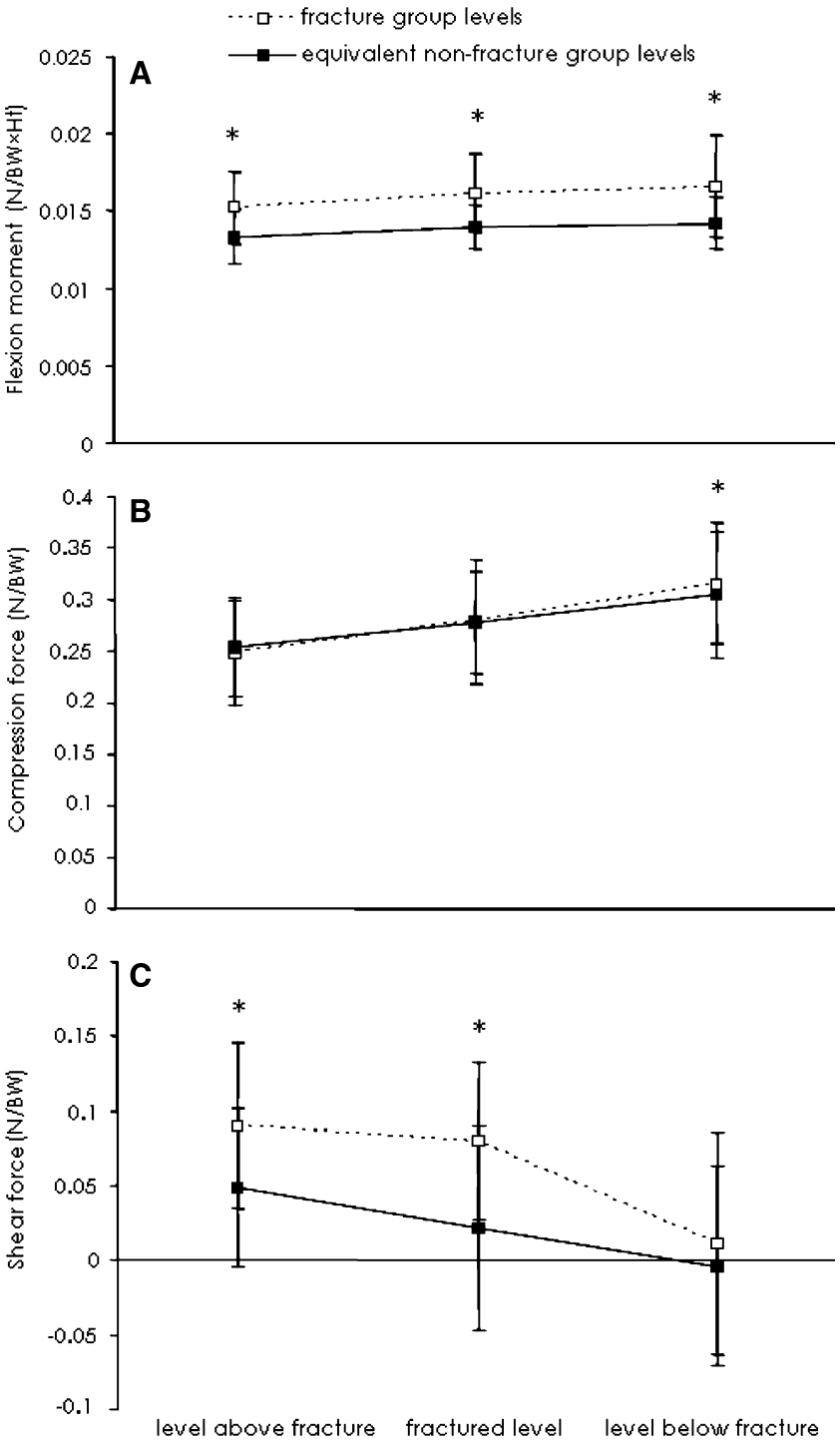

Fig. 6 Differences in normalised flexion moment (**a**), compression force (**b**) and shear force (**c**) between individuals with fractures compared to the non-fracture group mean at the level of fracture and one level above and below. Symbol *asterisk* denotes significant differences ($p < 0.05$, 2-tailed) between groups. *Error bars* indicate 1SD

participants in the fracture group sustained a single vertebral fracture. Thus, a single vertebral fracture is unlikely to significantly change thoracic kyphosis when measured with conventional radiographic tools, in agreement with previous work [28]. However, a single fracture is responsible for a subtle change in curvature, sufficient to significantly increase loading. Recent evidence suggests than an increase in sagittal curvature operates as a significant and independent predictor of future fracture [30]. Interventions to minimise spinal loads should therefore be implemented immediately after a vertebral fracture to offset the risk of further fracture.

Models examining load profiles in spines with pathology are rare. Fracture-induced changes in vertebral morphology occur due to decreased trabecular bone strength as a consequence of the pathophysiology of osteoporosis resulting in reduced bone mass.

Specifically, trabecular bone mass in the central and anterior zones of the vertebral body becomes reduced relative to other intra-vertebral zones [7, 46]. However, vertebral fractures and the high risk of subsequent fractures cannot be explained solely by low bone mass [32]. Indeed, results in this study demonstrate the presence of a fracture to be associated with greater loading profiles in the thoracolumbar spine. It is likely that the increased load profiles in fracture cases are a result of the fracture and the consequential changes in vertebral morphology. This may help to explain, in part, a mechanism of the increased risk of subsequent fracture after an initial fracture.

Wedge fractures change vertebral morphology by reducing anterior vertebral height and increasing the angle of superior endplate tilt. Consequently, the composite mass of the superior vertebral levels, head and arms may translate slightly anteriorly. The moment arm distance between the vertebral centroid and composite COM will increase, thereby increasing the flexion moment at that level, and contiguous levels. This theory is supported by our results where the flexion moment at the participant's level of fracture, and those adjacent to it, was greater compared to the flexion moment at the equivalent level of the non-fracture group. Initial fractures appear to be responsible for systematically greater flexion moments observed in the fracture group. The fracture-induced changes in vertebral morphology causing greater flexion moments locally and in adjacent vertebral levels may perpetuate morphologic changes and increase subsequent fracture risk. Contributions of vertebral geometry [24], densitometry [4] and bone quality characteristics [1, 41] in individuals with fractures are also likely to account for some of this increased risk. Shear forces were greater at the level of fracture and one level above, while compression forces were greater at one level below in the fracture compared to equivalent level mean forces of the non-fracture group. These results strongly suggest that the presence of an initial vertebral fracture is associated with increased loads locally and in adjacent levels, in agreement with a previous study [43]. It is likely therefore that altered load profiles in fracture cases increase the likelihood of subsequent fracture at contiguous segments.

The pattern of gradual increase in compression force values between T1 and L5 is consistent and in close agreement with findings from a previous study [13]. However, Keller et al. [34] reported a greater peak compression force (exceeding 842 N at T11/T12), compared to the mean, raw peak force in the current study of 388.8 ± 105.6 N (range: 228.6–695.5 N) at L4. The greater compression force in the Keller et al. [34] study may be attributable to greater body mass (mean 76.6 kg) of their participants, more significant vertebral deformities imposed onto their model, and relatively smaller shear forces. Compression force peaked in their study at T11/T12, compared to L4 in our study and previous studies [13, 18]. Although net compression forces were not different between groups at the level of fracture, compression force in the fracture group exceeded that of non-fracture cases at the level below the fracture. These findings are likely to be due to endplate tilt in the fracture group being greater, leading to increased shear forces compared to compression forces.

Mean shear force profiles were greater in the fracture group, peaking at the upper-mid thoracic spine and thoracolumbar junction. This lends support to the high fracture and subsequent fracture rate in these areas, and agrees with a previous study examining segmental shear loads in spines with osteoporosis [34]. The higher shear force profiles in the fracture group may be explained by their larger endplate angles, thereby creating larger shear force vectors, specifically at the level of fracture. Keaveny et al. [33] noted that from a strength perspective, trabecular bone properties are anisotropic. Trabecular bone has a lower strength in shear force compared to compression [21]. Therefore increased shear loading in the fracture group may help to explain an increased risk of subsequent vertebral fracture in this group. A recent study revealed that trabeculae in osteoporotic vertebrae withstand significantly greater strains than trabeculae of healthy vertebrae when loading was applied in a shear-like manner, suggesting that loading of this nature may increase the risk of vertebral failure [29].

This study is limited by the fact that the calculated moments and forces relate only to a standing posture. Future studies should investigate loading patterns in dynamic and functional activities for this population. The anatomic model used in the study was comprehensive for the lumbar spine, but only included paraspinal musculature for the thoracic levels. Optimization models have been validated in the past using EMG, but not in a population with osteoporosis. Therefore future research may use EMG to validate this model and examine the influence of antagonist activation in a comparable population.

Results from this study suggest that vertebral morphology has a significant influence on segmental loading thereby lending biomechanical support to interventions to restore normal vertebral architecture and spinal curvature such as vertebroplasty [12, 19]. Fracture-induced increases in segmental loading profiles may help to explain mechanisms underlying

the fracture cascade. Ultimately, distinguishing load characteristics before and after an initial fracture using a longitudinal design may elucidate mechanisms underlying initial vertebral fractures.

Acknowledgments The authors gratefully acknowledge the assistance of Associate Professor David Pearsall (McGill University, Canada) with providing additional trunk inertial data and the Medical Imaging department at St. Vincent's Hospital, Melbourne, Australia.Funding: seeding grant 013/05: Physiotherapy Research Foundation (Australia).

References

1. Aaron JE, Shore PA, Shore RC et al (2000) Trabecular architecture in women and men of similar bone mass with and without vertebral fracture II. Three-dimensional histology. Bone 27:277–82
2. Alexeeva L, Burckhardt P, Christiansen C et al (1994) Report of a World Health Organization study group. Assessment of fracture risk and its application to screening for postmenopausal osteoporosis. WHO, Geneva
3. Black DM, Arden NK, Palermo L et al (1999) Prevalent vertebral deformities predict hip fractures and new vertebral deformities but not wrist fractures. Study of osteoporotic fractures research group. J Bone Miner Res 14:821–828
4. Briggs A, Wark J, Phillips B et al (2005) Subregional bone mineral density characteristics in the lumbar spine: an in vivo pilot study using dual energy X-ray absorptiometry. Annual scientific meeting of the Australian and New Zealand bone and mineral society, Perth, Australia, 7–9 September 2005
5. Briggs AM, Greig AM, Wark JD et al (2004) A review of anatomical and mechanical factors affecting vertebral body integrity. Int J Med Sci 1:170–180
6. Briggs AM, Tully EA, Adams PE et al (2005) Vertebral centroid and Cobb angle measures of thoracic kyphosis. Intern Med J 35:A96
7. Briggs AM, Wark JD, Kantor S et al (2006) Bone mineral density distribution in thoracic and lumbar vertebrae: an ex vivo study using dual energy X-ray absorptiometry. Bone 38:286–288
8. Bürklein D, Lochmuller EM, Kuhn V et al (2001) Correlation of thoracic and lumbar vertebral failure loads with in situ vs. ex situ dual energy X-ray absorptiometry. J Biomech 34:579–587
9. Crowninshield RD, Brand RA (1981) A physiologically based criterion of muscle force prediction in locomotion. J Biomech 14:793–801
10. Dieën JHv (1997) Are recruitment patterns of the trunk musculature compatible with a synergy based on maximization of endurance? J Biomech 30:1095–1100
11. Dieën JHv, Kingma I (2005) Effects of antagonistic co-contraction on differences between electromyography based and optimization based estimates of spinal forces. Ergonomics 48:411–426
12. Dublin AB, Hartman J, Latchaw RE et al (2005) The vertebral body fracture in osteoporosis: restoration of height using percutaneous vertebroplasty. Am J Neuroradiol 26:489–492
13. Duval-Beaupere G, Robain G (1987) Visualization of full spine radiographs of the anatomical connections of the centres of the segmental body mass supported by each vertebra and measured in vivo. Int Orthop 11:261–269
14. Ebbesen EN, Thomsen JS, Beck-Nielsen H et al (1999) Lumbar vertebral body compressive strength evaluated by dual-energy X-ray absorptiometry, quantitative computed tomography, and ashing. Bone 25:713–724
15. Eckstein F, Fischbeck M, Kuhn V et al (2004) Determinants and heterogeneity of mechanical competence throughout the thoracolumbar spine of elderly women and men. Bone 35:364–374
16. Edmondston SJ, Singer KP, Day RE et al (1994) In-vitro relationships between vertebral body density, size, and compressive strength in the elderly thoracolumbar spine. Clin Biomech 9:180–186
17. Edmondston SJ, Singer KP, Day RE et al (1997) Ex vivo estimation of thoracolumbar vertebral body compressive strength: the relative contributions of bone densitometry and vertebral morphometry. Osteoporos Int 7:142–148
18. El-Rich M, Shirazi-Adl A, Arjmand N (2004) Muscle activity, internal loads, and stability of the human spine in standing postures: combined model and in vivo studies. Spine 29:2633–2642
19. Farooq N, Park JC, Pollintine P et al (2005) Can vertebroplasty restore normal load-bearing to fractured vertebrae? Spine 30:1723–1730
20. Felsenberg D, Boonen S (2005) The bone quality framework: determinants of bone strength and their interrelationships, and implications for osteoporosis management. Clin Ther 27:1–11
21. Ford CM, Keaveny TM (1996) The dependence of shear failure properties of trabecular bone on apparent density and trabecular orientation. J Biomech 29:1309–1317
22. Gardner-Morse MG, Laible JP, Stokes IAF (1990) Incorporation of spinal flexibility measurements into finite element analysis. J Biomech Eng 112:481–483
23. Genant HK, Jergas M (2003) Assessment of prevalent and incident vertebral fractures in osteoporosis research. Osteoporos Int 14:S43–S55
24. Gilsanz V, Loro LM, Roe TF et al (1995) Vertebral size in elderly women with osteoporosis: mechanical implications and relationships to fractures. J Clin Invest 95:2332–2337
25. Goh S, Price RI, Leedman PJ et al (2000) A comparison of three methods for measuring thoracic kyphosis: implications for clinical studies. Rheumatology 39:310–315
26. Hansson T, Roos B, Nachemson A (1980) The bone mineral content and ultimate compressive strength of lumbar vertebrae. Spine 5:46–55
27. Harrison DE, Cailliet R, Harrison DD et al (2001) Reliability of centroid, Cobb, and Harrison posterior tangent methods: which to choose for analysis of thoracic kyphosis. Spine 26:E227–E234
28. Hedlund LR, Gallagher JC, Meeger C et al (1989) Change in vertebral shape in spinal osteoporosis. Calcif Tissue Int 44:168–172
29. Homminga J, Van-Rietbergen B, Lochmuller EM et al (2004) The osteoporotic vertebral structure is well adapted to the loads of daily life, but not to infrequent error loads. Bone 34:510–516
30. Huang MH, Barrett-Connor E, Greendale GA et al (2006) Hyperkyphotic posture and risk of future osteoporotic fractures: the Rancho Bernado study. J Bone Miner Res 21:419–423
31. Jensen RK, Fletcher P (1994) Distribution of mass to the segments of elderly males and females. J Biomech 27:89–96
32. Kanis JA (2002) Assessing the risk of vertebral osteoporosis. Singapore Med J 43:100–105
33. Keaveny TM, Morgan EF, Niebur GL et al (2001) Biomechanics of trabecular bone. Annu Rev Biomed Eng 3:307–333

34. Keller TS, Harrison DE, Colloca CJ et al (2003) Prediction of osteoporotic spinal deformity. Spine 28:455–462
35. Keller TS, Holm SH, Hansson TH et al (1990) The dependence of intervertebral disc mechanical properties on physiologic conditions. Spine 15:751–761
36. Klotzbuecher CM, Ross PD, Landsman PB et al (2000) Patients with prior fractures have an increased risk of future fractures: a summary of the literature and statistical synthesis. J Bone Miner Res 15:721–739
37. Kopperdahl DL, Pearlman JL, Keaveny TM (2000) Biomechanical consequences of an isolated overload on the human vertebral body. J Orthop Res 18:685–690
38. Lindsay R, Silverman SL, Cooper C et al (2001) Risk of new vertebral fracture in the year following a fracture. JAMA 285:320–323
39. McCloskey EV, Spector TD, Eyres KS et al (1993) The assessment of vertebral deformity: a method for use in population studies and clinical trials. Osteoporos Int 3:138–147
40. Motulsky H, Christopoulos A (2003) Fitting models to biological data using linear and non-linear regression: a practical guide to curve fitting. GraphPad Software Inc., San Diego
41. Oleksik A, Ott SM, Vedi S et al (2000) Bone structure in patients with low bone mineral density with or without vertebral fractures. J Bone Miner Res 15:1368–1375
42. Pearsall DJ, Reid JG, Livingston LA (1996) Segmental inertial parameters of the human trunk as determined from computed tomography. Ann Biomed Eng 24:198–210
43. Rohlmann A, Bergmann G, Graichen F (1999) Loads on internal spinal fixators measured in different body positions. Eur Spine J 8:354–359
44. Ross PD, Davis JW, Epstein RS et al (1991) Pre-existing fractures and bone mass predict vertebral fracture incidence in women. Ann Intern Med 114:919–923
45. Ross PD, Genant HK, Davis JW et al (1993) Predicting vertebral fracture incidence from prevalent fractures and bone density among non-black, osteoporotic women. Osteoporos Int 3:120–126
46. Simpson EK, Parkinson IH, Manthey B et al (2001) Intervertebral disc disorganisation is related to trabecular bone architecture in the lumbar spine. J Bone Miner Res 16:681–687
47. Singer K, Edmondston S, Day R et al (1995) Prediction of thoracic and lumbar vertebral body compressive strength. Correlations with bone mineral density and vertebral region. Bone 17:167–174
48. Stokes IAF, Gardner-Morse M (1999) Quantitative anatomy of the lumbar musculature. J Biomech 32:311–316
49. Winter DA (1990) Biomechanics and motor control of human movement, 2nd edn. Wiley, New York